Available online at www.sciencedirect.com

SciVerse ScienceDirect

Ceramics International 38 (2012) 5195–5200

CERAMICS INTERNATIONAL

www.elsevier.com/locate/ceramint

Synthesis of zirconium diboride platelets from mechanically activated $ZrCl_4$ and B powder mixture

Shuqi Guo [a,*], D.H. Ping [b], Yutaka Kagawa [a,c]

[a] Hybrid Materials Unit, National Institute for Materials Science, 1-2-1 Sengen, Tsukuba, Ibaraki 305-0047, Japan
[b] High Temperature Materials Unit, National Institute for Materials Science, 1-2-1 Sengen, Tsukuba, Ibaraki 305-0047, Japan
[c] Research Center for Advanced Science and Technology, The University of Tokyo, 4-6-1 Komaba, Meguro-ku, Tokyo 153-8505, Japan

Received 14 January 2012; received in revised form 9 March 2012; accepted 9 March 2012
Available online 17 March 2012

Abstract

ZrB_2 platelets were prepared by mechanochemical processing a zirconium (IV) chloride–boron mixture with subsequent annealing from 800 °C to 1200 °C. The phases present were identified by X-ray diffraction. The size and morphology of the synthesized ZrB_2 powders were characterized by scanning electron and transmission electron microscopy. At 800 °C, ZrO_2 was detected in absence of ZrB_2. At or above 1000 °C, $ZrCl_4$–B converted to ZrB_2. Moreover, at 1200 °C, $ZrCl_4$–B completely converted to ZrB_2 without trace quantities of residual ZrO_2. The synthesized ZrB_2 consisted of platelets with a diameter of 0.1–2.1 μm and a thickness of 40–200 nm.

Keywords: Zirconium diboride platelets; Zirconium chloride; Boron; High-energy ball milling

1. Introduction

Zirconium diboride (ZrB_2) is one of the most important members of the family of ultra-high temperature ceramics. It has an extremely high melting point, high thermal and electrical conductivities, chemical inertness against many molten metals, excellent thermal shock resistance and relatively low density [1,2]. As a result, ZrB_2 ceramics are being considered for a variety of high-temperature (>1800 °C), thermomechanical and structural applications, such as furnace elements, plasma-arc electrodes and thermal protection structures for leading-edge parts on hypersonic re-entry space vehicles [1–5]. However, to meet the strict constraints of such structural applications, ZrB_2 ceramic materials require an improvement in strength, fracture toughness and resistance to oxidation. In particular, the use of ZrB_2 ceramic materials, even fully densified, in structural applications is limited by their poor resistance to fracture.

Early studies with Si_3N_4 and/or SiC demonstrated that the developed platelets and/or elongated grains in the fine matrix grains led to improved strength and fracture toughness [6–8]. Recently, Wu et al. prepared a ZrB_2–$MoSi_2$ composite with elongated ZrB_2 grains by reactive hot pressing at 1800 °C using Zr, Si, B and Mo as raw materials [9]. In addition, Zou et al. densified elongated ZrB_2 grains containing ZrB_2–SiC–WC composites by pressureless sintering ZrB_2, SiC and WC powder mixtures at 2200 °C [10]. The presence of elongated ZrB_2 grains significantly improved the fracture toughness of these materials [9,10]. Hence, the motivation of this study was the development of ZrB_2 platelets and ZrB_2 ceramics with elongated grains.

Currently, Khanra et al. [11] synthesized ZrB_2 whiskers by heating a mixture of ZrO_2, H_3BO_3 and C with Ni, Co and Fe catalysts in a Ar atmosphere between 1300 °C and 1700 °C. However, various defects were observed in the resulting ZrB_2 whiskers. Very recently, Hu et al. [12] prepared plate-like ZrB_2 grains at 1550 °C by a solid–liquid reaction using Zr and B powders with Mo and Si catalysts. These studies have demonstrated that we can achieve the synthesis of platelets and/or elongated ZrB_2 grains by selecting appropriate compositions and synthetic methods. Mechanochemical processing is another attractive method for synthesizing materials. The authors prepared nanosized ZrB_2 powders by the mechanochemical processing of a ZrH_2–B mixture [13].

* Corresponding author. Tel.: +81 29 859 2223; fax: +81 29 859 2401.
E-mail address: GUO.Shuqi@nims.go.jp (S. Guo).

0272-8842/$36.00
doi:10.1016/j.ceramint.2012.03.026

In the present study, the ZrB_2 platelets were prepared by the mechanochemical processing of a zirconium (IV) chloride–boron mixture and subsequent annealing between 800 °C and 1200 °C. The phases present in the resulting platelets were identified by X-ray diffraction (XRD). The microstructure was characterized by scanning electron and transmission electron microscopy (SEM and TEM). In addition, the effects of annealing temperature on particle size and morphology were discussed.

2. Experimental

The starting powders used in this study were zirconium (IV) chloride ($ZrCl_4$) (99.5% pure, Strem Chemicals, Newburyport) and amorphous boron (B) ($d_{50} = 0.8$ μm, 95.9% pure, H.C. Starck). Fig. 1 shows SEM images of the as-received $ZrCl_4$ and amorphous B powders. The $ZrCl_2$ powder had large and angular with a particle size range of 0.8–3.1 μm, whereas B consisted of smaller, spherical particles. The minimum amount of B in the initial powder mixture was obtained according to the following stoichiometric reaction:

$$3ZrCl_4 + 10B \rightarrow 3ZrB_2 + 4BCl_3 \quad (1)$$

Then, B was generally added in excess (50 wt.%) to the stoichiometric content.

The $ZrCl_4$ and B powders were mixed in an agate mortar in ambient air to a homogeneous mass. Subsequently, the as-received $ZrCl_4$–B mixture was milled using a high-energy, planetary ball mill (Model P5, Fritsch Gmbh) using stainless steel balls with a diameter 9.5 mm and stainless steel vials with an inside diameter of 65 mm and an inside height of 45 mm. The ball to powder weight ratio was 20:1, and the milling speed was 300 rpm. To synthesize high-purity ZrB_2, milling was conducted under a Ar atmosphere without interruption for 2 h and 5 h. After milling, the powder was transferred to an alumina crucible under a Ar atmosphere in a glove box. Then, the post-milled powders were annealed between 800 °C and 1200 °C with a heating rate of 5 °C/min for 1 h in a flowing Ar atmosphere. Field-emission scanning electron microscopy (FE-SEM) was performed to characterize the evolution of the platelet size and morphology as a function of temperature. The microstructure of the powders was investigated by TEM (JEOL JEM-2010F) operated at 200 kV. XRD analysis was used to determine the phases present in the prepared powders. In addition, the average crystallite size of ZrB_2 was calculated using Scherrer's formula [14] and the (1 0 1) and (1 0 0) reflections.

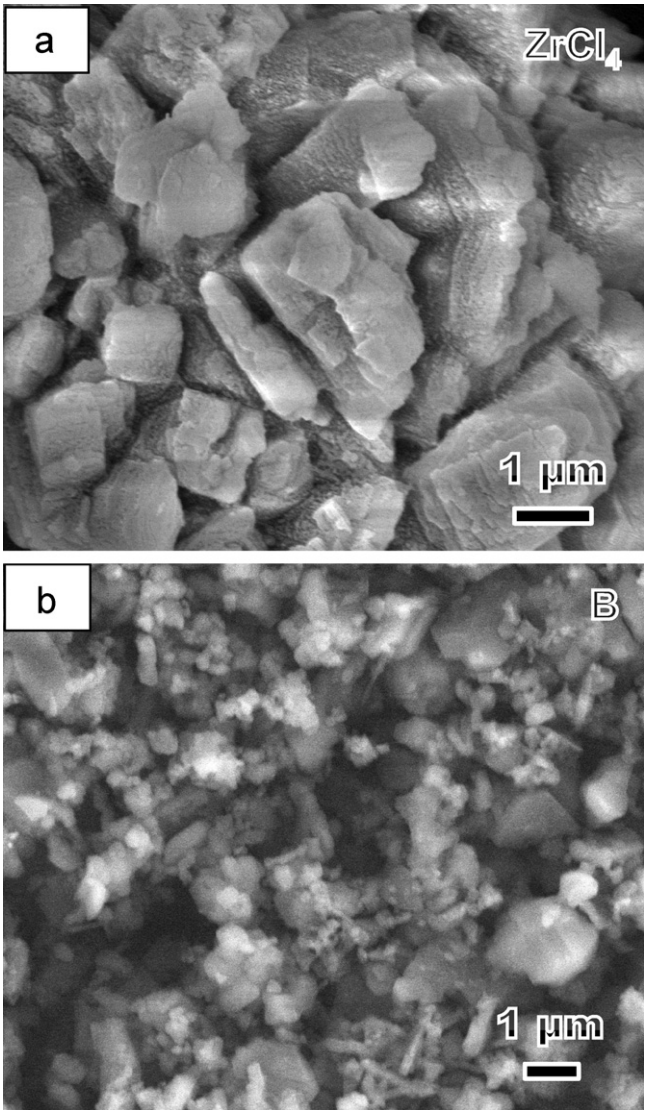

Fig. 1. Typical FE-SEM images of the as-received (a) $ZrCl_4$ and (b) B powders.

3. Results and discussion

Fig. 2 shows the XRD patterns obtained in ambient atmosphere for the as-received $ZrCl_4$–B mixture. The very broad XRD peaks in the starting $ZrCl_4$ are the result of air hydration. The peaks correspond to those of $ZrOCl_2{\cdot}nH_2O$ ($0 \leq n \leq 8$), which is the product of the hydration of $ZrCl_4$ in air rather than $ZrCl_4$. It is known that $ZrCl_4$ is very hygroscopic and easily hydrates and reacts with water to form $ZrOCl_2$ immediately on contact with air by the following reaction:

$$ZrCl_4 + H_2O \rightarrow ZrOCl_2 + 2HCl \quad (2)$$

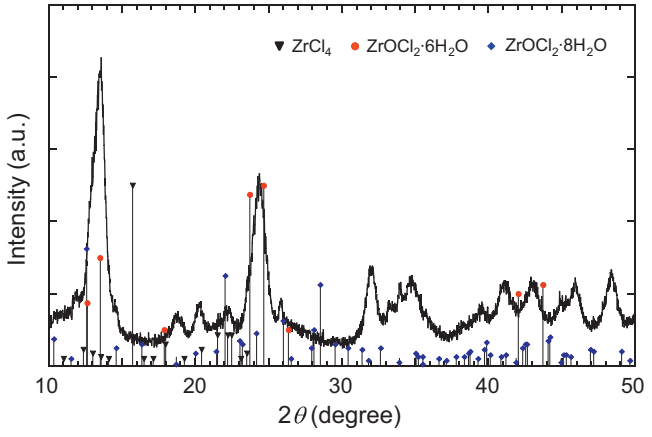

Fig. 2. X-ray diffraction patterns of the as-received $ZrCl_4$–B mixture powder.

Then, $ZrOCl_2$ continues to hydrate up to $ZrOCl_2{\cdot}8H_2O$. Even though $ZrCl_4$ is only in contact with air, slower hydrolysis reactions may also occur and lead to the formation of $ZrOCl_2{\cdot}nH_2O$ with a hydration content of n $(0 < n \leq 8)$, depending on the temperature, vapour pressure and contact time. An earlier study [15] showed that after partial hydration in air, $ZrCl_4$ forms cores surrounded by an outer shell of hydrated zirconium oxychloride. In the present study, because the powder is stored in a box that has to contact with air or air moisture, thus the starting $ZrCl_4$ powder is presumably hydrated and consists of $x ZrCl_4$–$(1-x)ZrOCl_2$–$2(1-x)HCl$–nH_2O with $0 < n \leq 8$. The primary products were identified to be $ZrOCl_2{\cdot}nH_2O$ ($n = 6$ or 8) from the XRD peaks (Fig. 2). However, excess B was not detected by XRD, because of its low atomic number and the fact that amorphous boron powder used.

Fig. 3 shows the XRD patterns of the powders annealed between 800 °C and 1200 °C. It is found that the reaction products of the post-milled precursors after annealing depended on temperature. At 800 °C, ZrO_2 is the primary crystalline phase, and Fe_2B is the minor phase; however, ZrB_2 was not detected. This indicated that only the thermal dehydration of zirconium oxide halide occurred, and the reaction for producing ZrB_2 did not occur at or below 800 °C. The trace quantities of Fe_2B may be attributed to iron uptake from the stainless steel vials and balls during the milling procedure. The dehydration of zirconium oxide halide during heating and/or isothermal heating is well documented in the literature. Powders and Gray [16] showed that $ZrOCl_2{\cdot}8H_2O$ dehydrated in a stepwise manner to the respective hexahydrate, tetrahydrate and finally ZrO_2 and that dehydration is complete at 700 °C. Li [17] synthesized a spherical ZrO_2 powder by the coagulation of colloidal particles in a zirconium aqueous sol followed by calcination at 650 °C using zirconium oxychloride as raw material.

On the other hand, in the powder annealed at 1000 °C, ZrB_2 was the primary crystalline phase, ZrO_2 was the secondary phase and trace amount of Fe_2B was present. This indicated that the ZrO_2 produced on heating reacted with B to form ZrB_2. Ran et al. [18] synthesized ZrB_2 powder by borothermal reduction of the starting powder mixture of ZrO_2, amorphous B and H_3BO_3 between 900 °C and 1650 °C in vacuum for 2 h. Their results showed that the crystalline ZrB_2 powder could be produced at or above 1000 °C via the following reaction:

$$3ZrO_2(s) + 10B(s) \rightarrow 3ZrB_2(s) + 2B_2O_3(l) \quad (3)$$

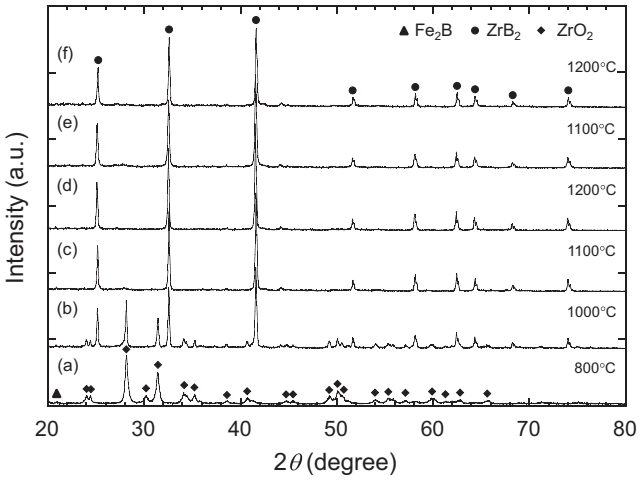

Fig. 3. X-ray diffraction patterns of the powders prepared by ball milling for (a–d) 2 h and (e, f) 5 h and annealing from 800 °C to 1200 °C.

Also, another study of the borothermal reduction of ZrO_2 and B powder mixture showed that ZrB_2 was prepared by the mechanochemical processing and subsequent annealing at 1100 °C instead of 1700–2000 °C without mechanical treatment [19]. The direct synthesis of ZrB_2 at lower temperatures was mainly attributed to the increased chemical mixing as well as concentration of defects in the ZrO_2 grains during milling. A similar explanation is favoured in this study because the ZrO_2 obtained upon heating of $ZrCl_4$ showed many defects [17].

The peak intensity of the ZrO_2 phase rapidly decreased with increasing annealing temperature. For the sample annealed at 1100 °C, only a trace quantity of ZrO_2 was detected. At 1200 °C, the peaks corresponding to ZrO_2 are non-existent, showing the absence of ZrO_2, because of the substantial reaction of ZrO_2 with B. The decrease in ZrO_2 suggests that the ZrO_2 detected in this study is a possible intermediate reaction product and resulted from the dehydration of zirconium oxide halides produced by the hydrolysis reaction of $ZrCl_4$ upon heating and/or isothermal heating. An early study regarding the synthesis of HfB_2 from mechanically activated $HfCl_4$ and B powder mixtures and subsequent annealing [20] showed that HfO_2 is an intermediate reaction product, and the amount of HfB_2 concomitantly increased with annealing time, which is accompanied by the decrease in HfO_2. Furthermore, the presence of HfO_2 is necessary for producing HfB_2. In addition, traces of Fe_2B are present in all annealed powders. The lattice parameters (Table 1) of the synthesized ZrB_2 phase are nearly

Table 1
Lattice parameters, crystallite size and size of the synthesized ZrB_2 platelets.

Powders	Mixture time (h)	Processing conditions	Lattice parameters (Å)		Platelet's size (μm)		Crystallite size (nm)
			a	*c*	*d*	*t*	
ZCB-1	2	1000 °C/60 min/Ar	3.165	3.535	0.1–1.4	0.04–0.2	49
ZCB-2	2	1100 °C/60 min/Ar	3.165	3.530	0.1–1.5	0.05–0.2	49
ZCB-3	2	1200 °C/60 min/Ar	3.169	3.532	0.2–1.8	0.06–0.2	50
ZCB-4	5	1100 °C/60 min/Ar	3.167	3.531	0.1–1.2	0.06–0.2	41
ZCB-5	5	1200 °C/60 min/Ar	3.167	3.531	0.2–2.1	0.07–0.2	46

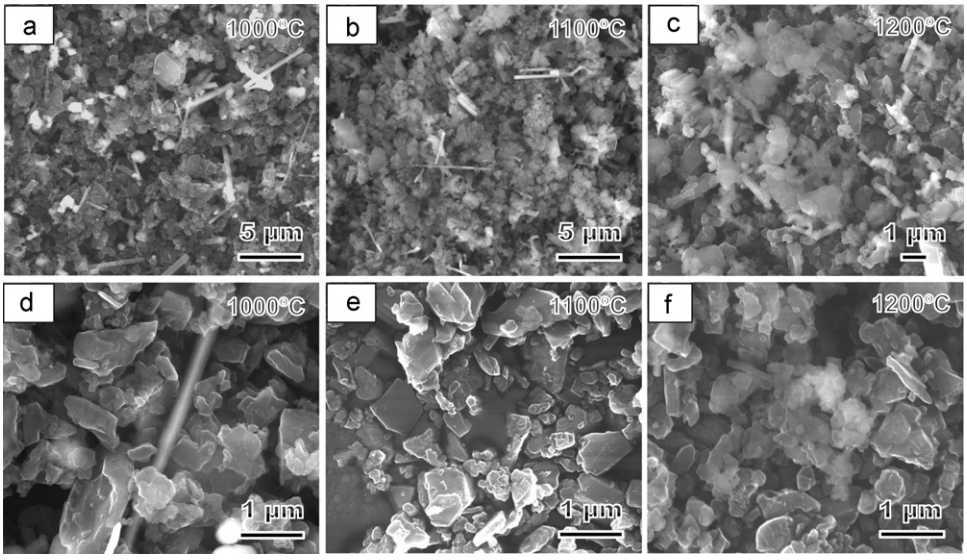

Fig. 4. Typical FE-SEM images of the powders prepared by ball milling for 2 h and annealing from 1000 °C to 1200 °C; (a–c) large scale overview and (d–f) top-view of platelets under high resolution.

identical to those of the pure hexagonal ZrB_2 phase ($a = 3.168$ Å, $c = 3.530$ Å, PDF#340423). For the sample milled for 2 h, the crystallite size calculated using Scherrer's formula was approximately 50 nm, regardless of the annealing temperature (Table 1). However, for the sample milled for 5 h, the crystallite size slightly increased with temperature and was found to be slightly smaller than that of the sample milled for 2 h.

The morphology of the ZrB_2 powders, prepared by the mechanochemical processing of the $ZrCl_4$–B mixture and annealing, was observed under FE-SEM, as shown in Fig. 4. The SEM observations showed the presence of platelet-like particles with diameters of 0.1–1.8 μm and thicknesses of approximately 40–200 nm. The morphologies of all post-annealed powders were similar, showing a bimodal particle size distribution. The increase in the annealing temperature led to small increase in the diameter of the platelets (Table 1). In addition, the particles size and morphology of the sample milled for 5 h was similar to those of the sample milled for 2 h (Fig. 5 and Table 1). This suggests that the particles size and morphology of the sample slightly depend on milling time. A study of the HfB_2 powders synthesized using $HfCl_4$–B powder mixture [20] showed that the morphology of HfB_2 depended on the composition of the starting mixture, regardless of milling time. Comparing these micrographs with the results determined by XRD (Table 1) revealed that the size of the ZrB_2 platelets determined by both techniques was markedly different. The platelet size observed by SEM is much larger than that determined by XRD. This suggests that the ZrB_2 platelets in this study are not single crystals but polycrystalline specimens with nanosized grains. Very recently, Hu et al. [12] directly prepared plate-like ZrB_2 grains by reacting Zr with B under Mo and Si catalysis at 1550 °C in flowing Ar atmosphere. They concluded that the formation of plate-like ZrB_2 grains is a result of the preferred growth of ZrB_2 grains along the *a*- or *b*-axis because of its low-activation energy diffusion path along the <2 1 0> and <1 1 0> directions [21].

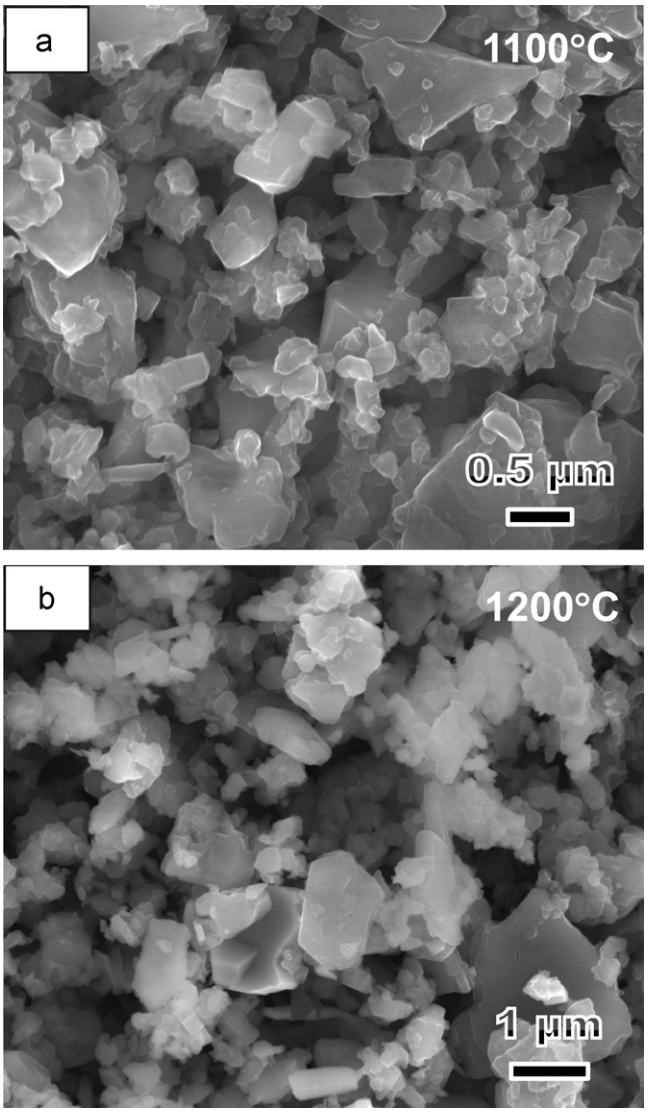

Fig. 5. Typical FE-SEM images of the powders prepared by ball milling for 5 h and annealing at 1100 °C (a) and 1200 °C (b).

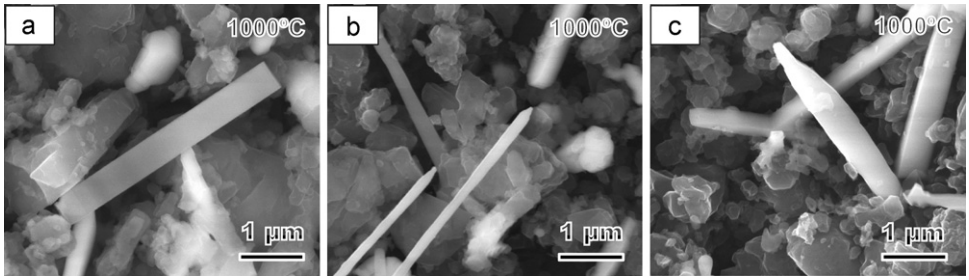

Fig. 6. FE-SEM images of the platelets prepared by ball milling and annealing (ZCB-1), showing whiskers with different morphologies: (a) rectangular, (b) needle and (c) rod.

In addition, some elongated and/or whisker-like ZrB_2 grains were observed among the prepared ZrB_2 platelets (Fig. 4). Under high-magnification (Fig. 6), it is clearly shown that the elongated ZrB_2 has three different morphologies: (i) rectangular, (ii) needle and (iii) rod. Khanra et al. [11] synthesized ZrB_2 whiskers from ZrO_2, H_3BO_3, C and NaCl with Ni, Co and Fe additives between 1300 °C and 1500 °C using the carbothermal synthesis technique. They showed that the addition of Fe favoured the formation of rod-shaped whiskers, which were grown by the combined vapour–solid and vapour–liquid–solid mechanism. Barraud et al. [20] prepared nanorods of HfB_2 from a mechanically activated $HfCl_4$–B powder mixture. They showed that the HfB_2 nanorods formed only in the presence of a Fe catalyst and the presence of Fe_2B and B_2O_3 favoured the formation of HfB_2 rods. The main formation mechanism of the nanorods is by a vapour–solid reaction. The mechanically activated process favours the synthesis of HfB_2 rods by inducing reactions or increasing the reactivity of powders and by homogeneously mixing the elements at the nanometer scale [22]. In the present study, Fe_2B was always detected by XRD (Fig. 3), and B_2O_3 was also present. Thus, it is presumed that the presence of Fe_2B and B_2O_3 led to the formation of the observed ZrB_2 whiskers by a vapour–solid reaction among the ZrB_2 platelets.

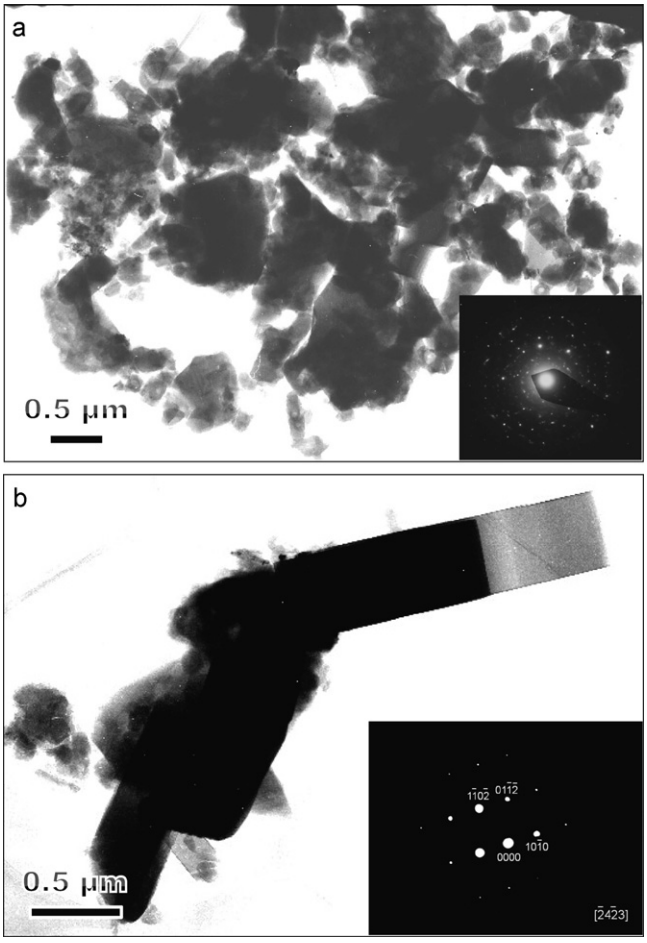

Fig. 7. Example of typical TEM images and the corresponding select area diffraction (SAD) patterns of the powders prepared by ball milling for 2 h and annealing at 1100 °C (ZCB-3), showing (a) platelet-shaped ZrB_2 polycrystals with nanosize grains and (b) needle-shaped ZrB_2 monocrystal.

Fig. 7 shows TEM images and the corresponding select area diffraction (SAD) patterns of the ZrB_2 powders prepared by ball milling for 2 h and annealing at 1100 °C. Here TEM showed that the particles of ZrB_2 were platelet-shaped. The smaller ZrB_2 platelets are polycrystalline and consist of nanosized grains (Fig. 7a). In addition, mainly ring type patterns having spots are found in the powders (Fig. 7a), indicating the presence of reasonably good nano-crystalline phases in the selected area. However, it is difficult to distinguish the larger ZrB_2 platelets because they are too thick for TEM observation. The nanosized ZrB_2 crystallites were in the range of 30–180 nm. The crystallite sizes estimated from the TEM micrographs are roughly consistent with those determined by XRD. In addition, the needle-shaped ZrB_2 particles are monocrystals (Fig. 7b). The formation of the monocrystals is the result of the preferred growth of ZrB_2 grains along the *c*-axis in the presence of Fe catalyst [20].

4. Conclusions

In summary, the platelet-like ZrB_2 particles were successfully prepared by the mechanochemical processing of a $ZrCl_4$–B mixture and subsequent annealing from 1000 °C to 1200 °C. ZrO_2 was identified as the possible intermediate reaction product. At 1000 °C, the $ZrCl_4$–B mixture transformed to ZrB_2 by a reaction between ZrO_2 and B that accompanied the hydrolysis reaction of $ZrCl_4$ following the dehydration of zirconium oxide halides to ZrO_2 upon heating. Trace quantities of unreacted ZrO_2 were detected at 1000 °C and 1100 °C. At

1200 °C, the $ZrCl_4$–B mixture completely converted to ZrB_2 without the presence of any residual ZrO_2. The resulting ZrB_2 powder consisted of platelet-like particles with a diameter of 0.1–2.1 μm, a thickness of 40–200 nm and traces of whiskers.

References

[1] K. Upadhya, J.-M. Yang, W.P. Hoffmann, Materials for ultrahigh temperature structural applications, Am. Ceram. Soc. Bull. 76 (1997) 51–56.

[2] S.Q. Guo, Densification of ZrB_2-based composites and their mechanical and physical properties: a review, J. Eur. Ceram. Soc. 29 (2009) 995–1011.

[3] A.S. Brown, Hypersonic designs with a sharp edge, Aerospace Am. 35 (1997) 20–21.

[4] S. Norasetthekul, P.T. Eubank, W.L. Bradley, B. Bozkurt, B. Stucker, Use of zirconium diboride-copper as an electrode in plasma applications, J. Mater. Sci. 34 (1999) 1261–1270.

[5] A. Blum, W. Ivanick, Recent developments in the application of transition metal borides, Powder Met. Bull. 7 (1956) 75–78.

[6] S.Q. Guo, N. Hirosaki, Y. Yamamoto, T. Nishimura, M. Mitomo, Improvement of high-temperature strength of hot-pressed sintering silicon nitride with Lu_2O_3 addition, Scripta Mater. 45 (2001) 867–874.

[7] H.J. Kleebe, G. Pezzotti, G. Ziegler, Microstructure and fracture toughness of Si_3N_4 ceramics: combined roles of grain morphology and secondary phase chemistry, J. Am. Ceram. Soc. 82 (1999) 1857–1867.

[8] G.D. Zhan, M. Mitomo, Y.W. Kim, Microstructural control for strengthening of silicon carbide ceramics, J. Am. Ceram. Soc. 82 (1999) 2924–2926.

[9] W.W. Wu, Z. Wang, G.J. Zhang, Y.M. Kan, P.L. Wang, ZrB_2–$MoSi_2$ composites toughened by elongated ZrB_2 grains via reactive hot pressing, Scripta Mater. 61 (2009) 316–319.

[10] J. Zou, G.J. Zhang, Y.M. Kan, Formation of tough interlocking microstructure in ZrB_2–SiC-based ultrahigh-temperature ceramics by pressureless sintering, J. Mater. Res. 24 (2009) 2428–2434.

[11] A.K. Khanra, L.C. Pathak, M.M. Godkhindi, Carbothermal synthesis of zirconium diboride whisker, Advances in Applied Ceramics 106 (2007) 155–160.

[12] C.F. Hu, J. Zou, Q. Huang, G.-J. Zhang, S.Q. Guo, Y. Sakka, Synthesis of plate-like ZrB_2 grains, J. Am. Ceram. Soc. 95 (2012) 85–88.

[13] S.Q. Guo, C.F. Hu, Y. Kagawa, Mechanochemical processing of nanocrystalline zirconium diboride powder, J. Am. Ceram. Soc. 94 (2011) 3643–3647.

[14] R. Jenkins, R.L. Synder, Diffraction theory. Introduction to X-ray powder diffractometry, John Wiley & Sons, New York, 1996, pp. 47–97.

[15] B. Beden, I. Guillaume, M.J. Martin, Properties of titanium and zirconium tetrachloride in ambient air, C. R. Acad. Sci. Ser. C 270 (1970) 34–36.

[16] D.A. Powers, H.B. Gray, Characterization of the thermal dehydration of zirconium oxide halide octahydrates, Inorg. Chem. 12 (1973) 2721–2726.

[17] M. Li, Making spherical zirconia particles from inorganic zirconium aqueous sols, Powder Technol. 137 (2003) 95–98.

[18] S. Ran, O. Van de Biest, J. Vleugels, ZrB_2 powders synthesis by borothermal reduction, J. Am. Ceram. Soc. 93 (2010) 1586–1590.

[19] P. Millet, T. Hwang, Preparation of TiB_2 and ZrB_2. Influence of a mechanochemical treatment on the borothermic reduction of titania and zirconia, J. Mater. Sci. 31 (1996) 351–355.

[20] E. Barraud, S. Bégin-Colin, G. Le Caër, Nanorods of HfB_2 from mechanically actived $HfCl_4$ and B-based powder mixtures, J. Alloys Compd. 398 (2005) 208–218.

[21] J. Zou, S.K. Sun, G.J. Zhang, Y.M. Kan, P.L. Wang, T. Ohji, Chemical reactions, anisotropic grain growth and sintering mechanism of self-reinforced ZrB_2–SiC doped with WC, J. Am. Ceram. Soc. 94 (2011) 1575–1583.

[22] C.C. Tang, Y. Bando, T. Sato, Oxide-assisted catalytic growth of MgO nanowires with uniform diameter distribution, J. Phys. Chem. B 106 (2002) 7449–7452.